Korean J. Chem. Eng., 34(10), 2780-2786 (2017)
DOI: 10.1007/s11814-017-0198-7

pISSN: 0256-1115
eISSN: 1975-7220

Performance evaluation of rotating photoelectrocatalytic reactor for enhanced degradation of methylene blue

Hyekyung Cho*,, Hyun Soo Seo*,**, Hyunku Joo*, Jong-Oh Kim**, and Jaekyung Yoon*,†**

*New and Renewable Energy Research Division, Hydrogen Laboratory, Korea Institute of Energy Research, 152 Gajeong-ro, Yuseong-gu, Daejeon 34129, Korea
**Department of Civil and Environmental Engineering, Hanyang University, 222 Wangsimni-ro, Seongdong-gu, Seoul 04763, Korea
(*Received 10 May 2017 • accepted 13 July 2017*)

Abstract−Enhanced oxidation of organic pollutant, methylene blue (MB) was conducted using a newly designed rotating photoelectrocatalytic process (PECP), compared with photocatalysis. A significant synergy of photoelectrocatalytic reaction was observed such that the degradation of methylene blue (MB) by the photoelectrocatalytic mode was 80% higher than that (61.6%) of photocatalytic mode. To confirm the potentials in the application of water treatment, the effects of various parameters affecting reaction performance were studied with the newly designed rotating photoelectrocatalytic reactor consisting of TiO_2 nanotubes and Ti lath as the photoanode and cathode, respectively, for applying electrical potential under UV irradiation. As the result of parameter studies, such as applied electrical potential (voltage), UV light intensity, rotating speeds, the highest degradation efficiencies of MB were achieved at 2.5 V or less (electrical potential), 90 rpm (rotating speed), and higher UV intensity. In addition, the stability and activity of TiO_2 nanotubes electrode were studied through repeated experiments and showed a good performance, excellent stability, and reliability in the rotating photoelectrocatalytic process (PECP). This study provides an basis for the development of a rotating PECP to water treatment.

Keywords: Photoelectrocatalytic Process (PECP), Rotating Reactor, TiO_2 Nanotubes, Photoanode, Water Treatment

INTRODUCTION

Among the advanced oxidation processes (AOPs), photocatalysis using semiconductor under UV or solar illumination is one of the attractive methods for water treatment. Extensive study has been performed to synthesize photocatalysts by various methods, characterize their properties, and measure their reactivity with various contaminants. Although photocatalysis has been extensively used in water treatment, the practical applications of the degradation of pollutants have been restricted and criticized, because of the inherent disadvantages such as catalyst recovery and a low photonic efficiency during the reaction [1-3].

To overcome the problem of catalyst recovery after the reaction, the fabrication of self-grown nanotubular TiO_2 on the substrate was considered as one of the immobilization strategies through the anodization technique, because of different geometric shapes and microstructure [4-8]. In our previous studies, various TiO_2 nanotubes were prepared on the various types of metal substrates (Ti foil or mesh) by anodization for the purposes of water-splitting hydrogen production [9-13] and photocatalytic water purification [14-17]. Particularly, we focused on developing self-rotating TiO_2 nanotubes to enhance the efficiency of photocatalytic Cr(VI) reduction and investigated the effect of the major parameters such as rotating speed and number of TiO_2 nanotubes on Cr(VI) reduction [15]. Moreover, the simultaneous treatment of Cr(VI) in the presence of endocrine disrupting compounds (EDCs) was investigated with the scale-up reactor system under solar UV irradiation. In extended outdoor tests, the synergistic effect of photocatalytic reduction and oxidation of inorganic Cr(VI) and EDCs (BPA, E2, and EE2) were confirmed by a stronger charge interaction and preventing recombination [17,18].

The fast recombination of electron-hole (e^--h^+) pairs, generated by photon energy, is a major obstacle in photocatalytic applications. Therefore, the decreased recombination rate of charge carriers is one of the solutions. Recently, the combination of electrochemical and photocatalytic methods, called as photoelectrocatalytic process, has began to attract wide attention, because of relatively high efficiency and large surface area than conventional photocatalysis [1,6-8]. The advantages of photoelectrocatalytic process provide the opportunity to separate the photogenerated electron holes and retard their recombination, allowing not only increasing the reaction efficiency, but also increasing the removal rate of pollutants [1-2,4,19]. In particular, anodized TiO_2 nanotubes on Ti substrate could directly be utilized as the electrode, easily composed of the photoelectrocatalytic system with the cathode under applied electrical potential [19-21].

The objective of this study was focused on the construction and development of a new rotating photoelectrocatalytic reactor, including the immobilized nanotubular TiO_2 electrodes to improve reaction performance by promoting the mass-transfer effect between

†To whom correspondence should be addressed.
E-mail: jyoon@kier.re.kr

photocatalyst and organic pollutant (methylene blue, MB). In particular, for the performance evaluation of this reactor, the effect of major parameters such as the distance between the photoanode and cathode, cathode materials, applied electrical potentials, UV intensity, number of photoanode, rotating speeds, and the stability of TiO_2 nanotube on the photoelectrocatalytic reaction were investigated by repeated tests. Through the experiments, a new rotating photoelectrocatalytic reactor may find its important possibilities and can be used in the various applications of water and wastewater treatment.

MATERIALS AND METHODS

1. Preparation of TiO_2 Nanotubular Photoanode

Prior to the anodization, the titanium (Ti) lath was chopped into pieces (100 cm^2, 1.67 mm thickness, SW (Short width) 3 mm, LW (Long width) 3 mm, 99% purity, TTM, Korea). The Ti lath was first pretreated with ethanol (Duksan, extra pure grade) and distilled water to remove the impurities and then etched by dipping into 0.5% hydrofluoric acid (HF, DC Chemical) solution for 1 min. The last pretreatment was repeatedly rinsed with distilled water and dried at room temperature.

The potentiostatic anodization was performed in a water-jacketed quartz bath connected to the power supply and controlled by a computer program (CIMON-SCADA, Korea). Iron (Fe) foil as the counter-electrode (100 cm^2, 0.25 mm thickness, 99.5% purity, Goodfellow, England) was used under magnetic stirring in the mixed chemicals composed of ammonium fluoride (0.3 M NH_4F)-water (2 vol% H_2O)-ethylene glycol ($C_2H_6O_2$). The TiO_2 nanotubes on Ti lath were then annealed at 450 °C for 2 hr under oxygen supply (400 mL/min). The prepared samples were cut into pieces (10 cm^2, 2 cm×5 cm) to adjust the number of nanotubular TiO_2 on Ti lath attached to the rotating axis of the photoelectrocatalytic reactor in accordance with the experimental conditions.

2. Chemicals

Ethylene glycol ($C_2H_6O_2$, 99.8%) and methylene blue trihydrate ($C_{16}H_{18}ClN_3$ $3H_2O$, 95%) were purchased from Duksan chemicals CO (Korea). Ammonium fluoride (NH_4F, ≥99.99%, Sigma-Aldrich, USA) was extra pure grade.

3. Experimental Set-up

A schematic diagram of the photoelectrocatalytic reactor and equipment is provided in Fig. 1. The photoelectrocatalytic reactor consisted of a tubular shape of quartz-reactor vessel, tetragonal rotating body including photoanodes and cathodes at each side connected and circuited via electrically external bias (power supply), and the UV lamp. The other parts of equipment included a digital flow-indicator, gear pump to control flowrate, tachometer to observe the rotating speed, radiometer to monitor the intensity

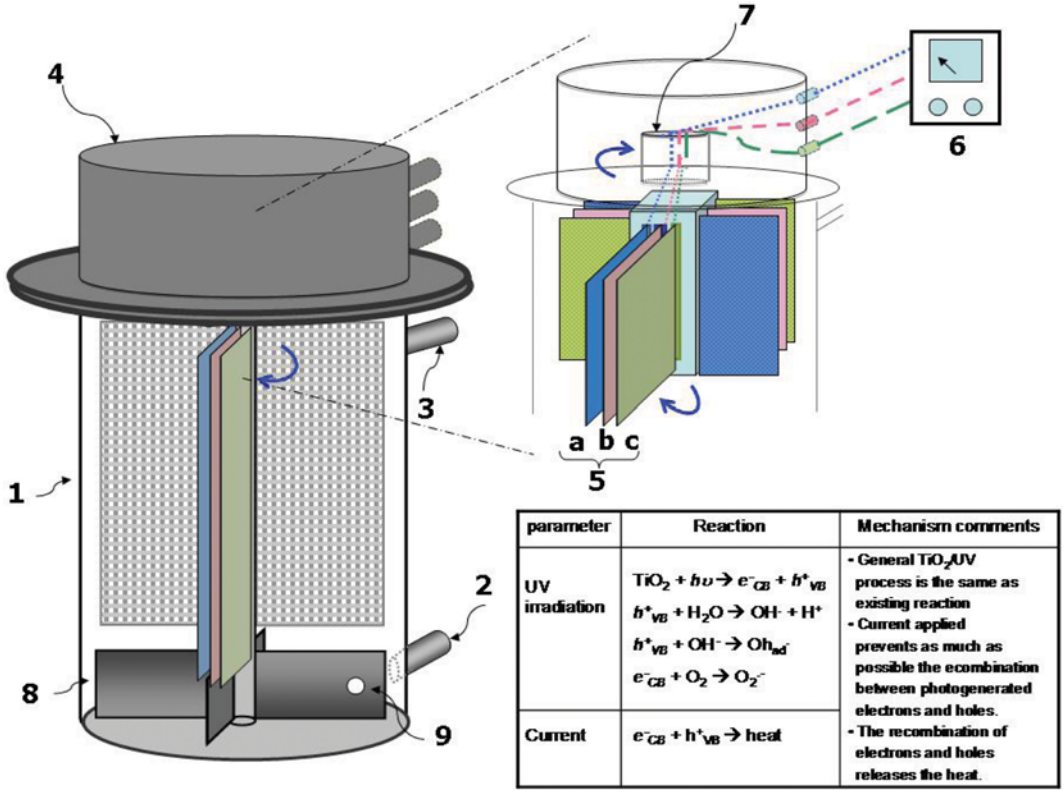

parameter	Reaction	Mechanism comments
UV irradiation	$TiO_2 + h\upsilon \rightarrow e^-_{CB} + h^+_{VB}$ $h^+_{VB} + H_2O \rightarrow OH^- + H^+$ $h^+_{VB} + OH^- \rightarrow Oh_{ad}$ $e^-_{CB} + O_2 \rightarrow O_2^-$	- General TiO_2/UV process is the same as existing reaction - Current applied prevents as much as possible the ecombination between photogenerated electrons and holes. - The recombination of electrons and holes releases the heat.
Current	$e^-_{CB} + h^+_{VB} \rightarrow$ heat	

Fig. 1. Representational illustration of the rotating photoelectrocatalytic reactor and reaction mechanisms.

1. Reactor vessel
2. Flow inlet
3. Flow outlet
4. Reactor cover
5a. Photoanode (TiO_2 nanotubes on Ti lath)
5b. Cathode
5c. Photoanodes (optional, in case of 8ea)
6. Power supply (source meter)
7. Ceramic bearing and slip-ring
8. 4-Blade impeller
9. Reflective tape for tachometer

from the UV light source.

First, the photoelectrocatalytic reactor with a total volume 1,000 mL was designed with an inner diameter, a quartz thickness, a length, and a volume of 7.7 cm, 3 mm, 12 cm, and 430 mL, respectively, in the presence of rotating body. The rotating body had impellers; its vertical axis was made of Teflon; and the fabricated photoanode (TiO_2 nanotubes on the Ti lath, 2 cm×5 cm, 1 or 2 pieces at each side, total 4 or 8 pieces at the 4 sides) and the cathode (Ti lath, 2 cm×5 cm, 1 piece in the middle at each side, total 4 pieces at the 4 sides) could be simply fixed into the hollows on the axis of the rotating body. The distance between the photoanode and cathode was 0.5 cm at all the sides. In addition, two pair of ceramic bearings were installed on the top and the bottom of the rotating body for easy rotation of the axis. The four-blade impellers were attached to the bottom side of the rotating axis, and the two types of electrodes (photoanodes and cathodes) were automatically rotated by inflow. The revolution speed depended on the inflow rate into the reactor, as measured by a tachometer (EE-2N, KONEX, Japan). Moreover, a source meter (KEITHLEY 2450, USA) connected between the photoanode and cathode onto the rotating body provided the electrical voltage and measured the current during the photoelectrocatalytic reaction.

A xenon lamp (1,000 W, Oriel, USA) equipped with an IR (infrared) filter was used as the light source. The emitted light wavelength was ≥300 nm, and the UV light intensity was an approximately 5,400 μW/cm^2 (300-400 nm, measured at 65 cm from the xenon lamp).

4. TiO_2 Nanotubes Characterization and MB Analysis

The structural properties of TiO_2 nanotubes on Ti lath before and after the repeated reactions were examined by SEM (Hitachi S-4700, Japan). The detailed characterization of SEM has been reported in our previous studies [17,18].

Photoelectrocatalytic properties were carried out in the three-electrode configuration. The properties of the TiO_2 nanotubes on Ti lath (photoanode) were monitored in the three-electrode cell configuration of the working electrode (WE, TiO_2 photoanode, 1 cm^2), counter electrode (CE, Ti lath, 1 cm^2), and reference electrode (RE, Ag/AgCl in 3 M NaCl). After the set-up of the three-electrode cell, the photoelectrochemical behavior was investigated by a potentiostat (ZIVE SP2, WonATech Co. Korea).

The quantitative analysis of MB was evaluated by UV-Visible spectrometry (SCINCO, S-3150, Korea). The sample solution (5 mL) containing MB was taken from the reservoir. Absorbance at 661 nm was measured in the wavelength range between 300 and 800 nm at a scan rate of 1 nm/s.

RESULTS AND DISCUSSION

1. Preliminary Experiments of MB Removal

Prior to the main experiments with the rotating photoelectrocatalytic reactor, preliminary tests were conducted to optimize the conditions such as the distance between the photoanode and cathode and the selection of cathodic materials (Fig. 2(a) and (b)). The total volume of the reactor was 200 mL; the pH and initial concentrations of the target compound were adjusted. The outside reactor was made of quartz and had a water jacket to maintain the

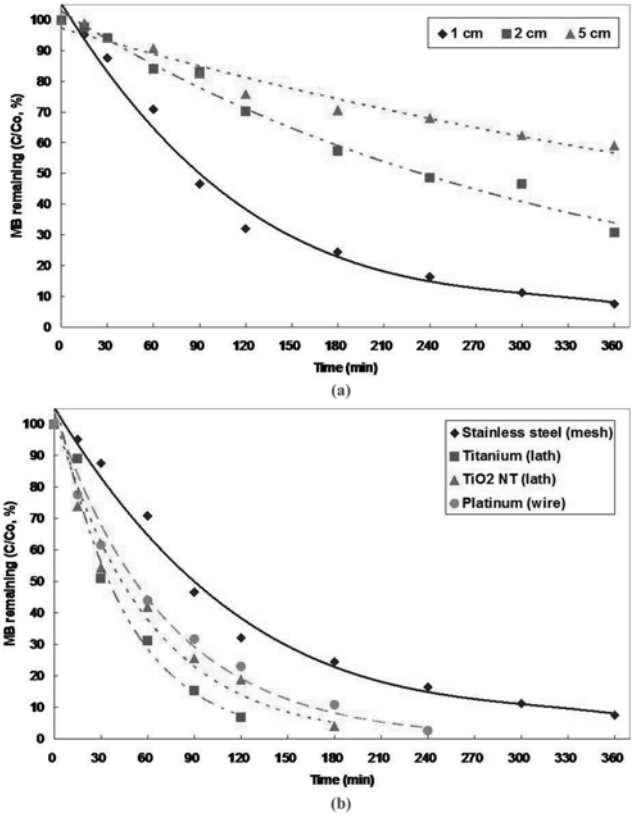

Fig. 2. Comparison of MB removal in the photoelectrocalytic experiments; (a) Effect of the distance between the photoanode (TiO_2 nanotubes on Ti lath) and cathode (stainless steel); (b) Effect of various cathode materials; ([MB]$_O$=5 ppm at pH 7, UV light intensity 5,400 μW/cm^2, external electrical potential applied 1.5 V, electrode area: 2 cm×5 cm, feed volume 200 mL).

reaction temperature [14]. The photoelectrocatalytic process utilized the various cathodes, made of reticulated vitreous carbon (RVC) [22], stainless steel [23,24] on which hydrogen peroxide, a beneficial by-product of water purification, can be separately generated in the reaction system [1,22,23].

Fig. 2(a) shows the effect of the distance between the two electrodes, TiO_2 nanotubes on Ti lath and stainless steel as the photoanode and the cathode, respectively, for the removal of MB. The two electrodes were fixed without movement by stirring flow before starting reaction. By changing the distance (1, 2, and 5 cm) between the two electrodes, the MB oxidation increase with decreasing distance as predicted [1]. Moreover, various metal substrates such as stainless steel (SS), titanium (Ti), TiO_2 nanotube (same as photoanode), and platinum were applied to select the optimum cathode material. In these experiments, the size of all the cathode materials except for the platinum wire was the same (2 cm×5 cm) as of photoanode. Fig. 2(b) shows the MB removal profile with different cathode materials. The efficiencies of MB removal are as follows: Ti (lath)>TiO_2 nanotubes on Ti lath>Pt (wire)>stainless steel (mesh). Platinum is well known to be one of the best materials. We used a wire type Pt electrode (Diameter×Length, 1 mm×7 cm), which was not comparable to other metal substrates because of different size and expensive material. From the results, the Ti

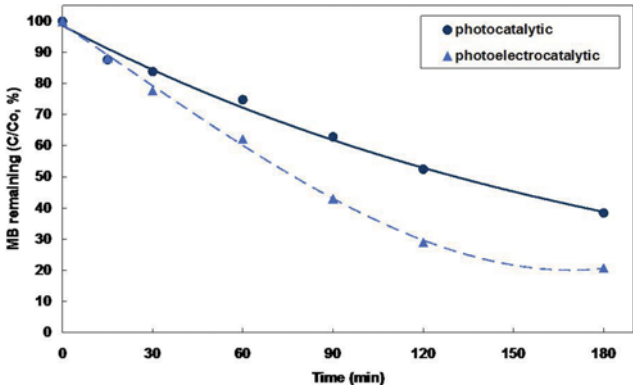

Fig. 3. Comparison of MB removal profiles under photocatalytic vs. photoelectrocatalytic modes ($[MB]_O$=2 ppm at pH 7, UV light intensity 5,400 μW/cm^2, external electrical potential applied 1.5 V, photoanode (TiO_2 nanotubes on Ti lath) and cathode (Ti) area: 2 cm×5 cm, feed volume 1,000 mL, the ratio of the number of photoanode : cathode=4 : 4).

lath showed a better performance, and the less distance between the two electrodes, and not the contact, was favorable for the photoelectrocatalytic reaction. The new rotating photoelectrocatalytic reactor was established based on these conditions.

2. Comparison of MB Removal under Photocatalysis vs. Photoelectrocatalysis in the Rotating Reactor

Fig. 3 shows the photocatalytic and photoelectrocatalytic oxidation, performed to compare the efficiency of MB oxidation, by the rotating reactor in Fig. 1. The photoelectrocatalytic oxidation of MB was conducted with photoanodes (TiO_2 nanotubes on Ti lath, 2 cm×5 cm, 4ea) and cathodes (Ti lath, 2 cm×5 cm, 4ea) at an electrical potential of 1.5 V, and a photocatalytic oxidation was performed with TiO_2 NT/Ti (the same number and size of photoanode) for comparison. As shown in Fig. 3, two reactions exhibit different trends and the MB degradation on the phoeoelectrocatalytic is faster than that in the photocatalytic mode.

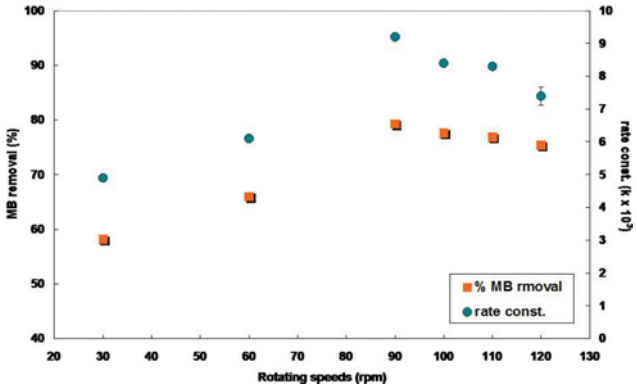

Fig. 4. Effect of rotating speeds in the range of 30 to 120 rpm on the MB removal and first-order rate constant in the photoelectrocatalytic mode modes ($[MB]_O$=2 ppm at pH 7, UV light intensity 5,400 μW/cm^2, applied electrical potential 1.5 V, photoanode (TiO_2 nanotubes on Ti lath) and cathode (Ti) area: 2 cm×5 cm, feed volume 1,000 mL, the ratio of the number of photoanode : cathode=4 : 4).

Table 1. Photoelectrocatalytic removal efficiencies and first-kinetic rate constant of MB at various rotating speeds with the couple of photoanode and cathode

Rotating speed (rpm)	$k_{oxid.}\times10^3$ (min^{-1})	Regression coefficients (R^2)
30	4.9	0.992
60	6.1	0.993
90	9.2	0.985
100	8.4	0.998
110	8.3	0.98
120	7.4	0.996

3. Effect of Rotating Speeds on MB Removal in the Photoelectrocatalytic Reactor

A series of photoelectrocatalytic experiments were conducted to remove MB at varying rotating speeds ranged from 30 rpm to 120 rpm. The relationship between the rotating speed to inflow rate and hydraulic retention time (*HRT*) was investigated in the previous studies and has been described in detail [15,17].

Fig. 4 and Table 1 represent the removal efficiencies and the first-order rate constant (k) of MB according to the rotating speeds (reaction time within 180 min). Moreover, the kinetic constant and regression coefficient (R^2) at each rotating speed were evaluated by linear fitting of the logarithmic plots, $\ln([MB]_o/[MB]_t)=kt$ (k is rate constant). The degradation of organic pollutants is well known to be in agreement with the first-order kinetics and was also confirmed in this photoelectrocatalysis [19,22,23].

These results show that the removal trend of MB was significantly associated with the rotating speed. Especially, the removal efficiency of MB was higher at 90 rpm. The rate constants (k) also showed a similar trend and matched with the removal efficiencies. These results indicate that the hydrodynamic conditions and mass transfer are significantly related to the rotating speed of the photoelectrocatalytic reactor. Therefore, organic contaminants have to be effectively transported to the surface of photoanode (TiO_2

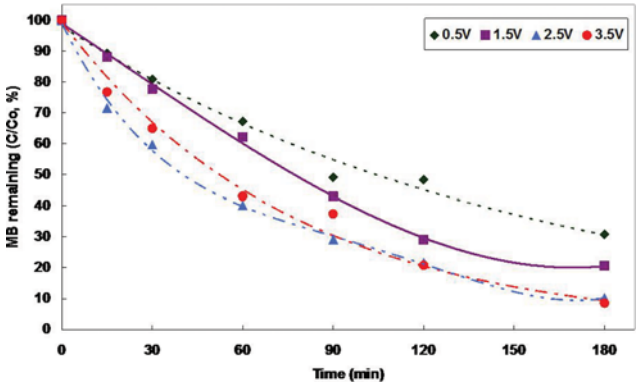

Fig. 5. Effect of applied electrical potential on the photoelectrocatalytic MB removal ($[MB]_O$=2 ppm at pH 7, UV light intensity 5,400 μW/cm^2, electrical potential applied 0.5-3.5 V, photoanode (TiO_2 nanotubes on Ti lath) and cathode (Ti) area: 2 cm×5 cm, feed volume 1,000 mL, the ratio of number of photoanode : cathode=4 : 4, rotating speed 90 rpm).

nanotubes on Ti lath), and then be oxidized by hydroxyl radicals or the generated hole onto/into the nanotubular TiO_2 [1,25-27]. Therefore, 90 rpm was the optimum rotating speed in this system and used for the subsequent tests.

4. Effect of External Potential Applied on MB Removal in Photoelectrocatalysis

Fig. 5 shows the results of photoelectrocatalytic MB oxidation at different applied potentials on the photoanode. The application of external potential on photoanode is known for the separation of the generated electron-hole by UV light, the prevention of charge recombination, and the increase of excited time of active holes. For these reasons, the hole excited in the photoelectrocatalytic process can directly to react with the organic contaminants on the surface of TiO_2 nanotubes on Ti lath or indirectly react with hydroxyl radicals.

As shown in Fig. 5, the external electrical potentials were applied to the photoanodes under UV illumination. The rate of MB degradation increases with increasing voltages in the range of 0.5-2.5 V. However, the removal efficiency of MB at 3.5 V was not improved. The effect of the external potential on pollutant treatment has been studied by many researchers [19,21-23,26]. According to these studies, the increasing external potential above the optimum voltage (or current) may decrease the removal efficiency, but also has a slight effect.

As shown in Fig. 6(a), linear sweep voltammetry (LSV) was performed to examine the photoelectrochemical activity of the photo-

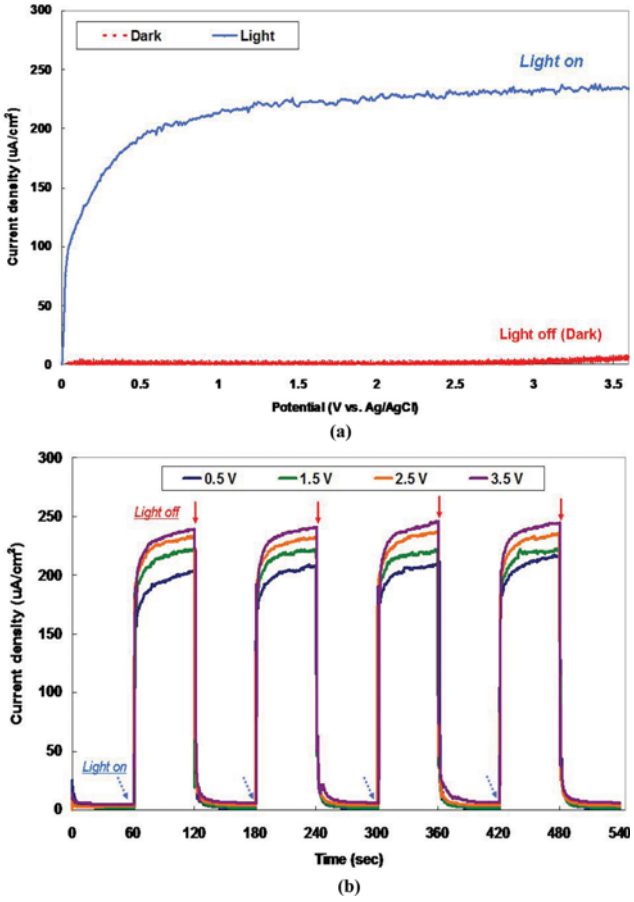

Fig. 6. Photoelectrochemical characterization of photoanode (TiO_2 nanotubes on Ti lath); (a) Linear sweep voltammetry (LSV) curves under light and dark conditions; (b) chronoamperometry curves at four different voltages (0.5-3.5 V *vs.* Ag/AgCl) under alternative light and dark conditions.

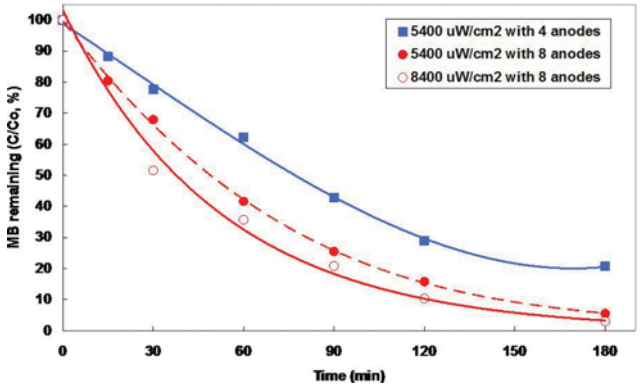

Fig. 7. Effect of the photoanode number and UV intensity on the photoelectrocalytic MB removal ($[MB]_O$=2 ppm at pH 7, conductivity 1,030 μS/cm, applied electrical potential 1.5 V, photoanode (TiO_2 nanotubes on Ti lath) and cathode (Ti) area: 2 cm×5 cm, feed volume 1,000 mL, rotating speed 90 rpm).

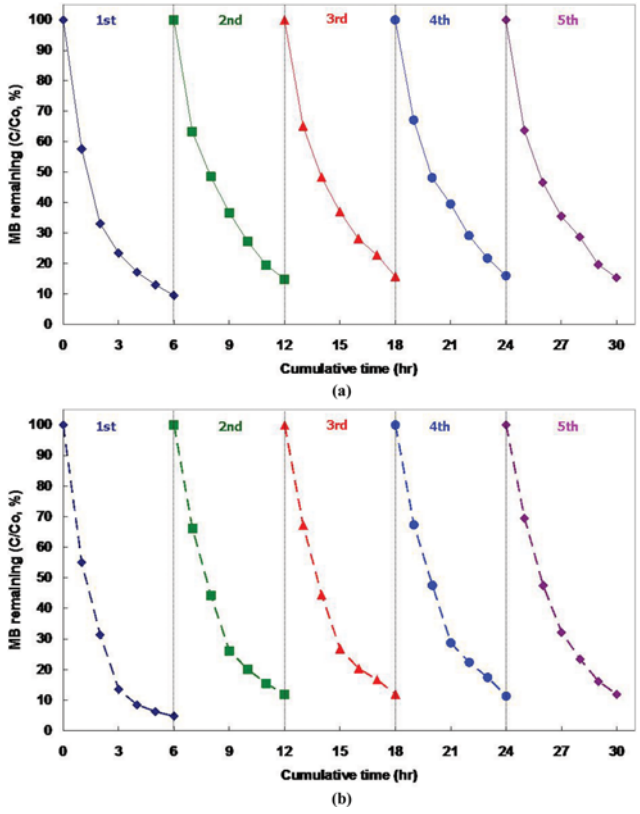

Fig. 8. MB removal of five repeated experiments in the photoelectrocatalytic reaction at (a) 1.5 V; and (b) 2.5 V ($[MB]_O$=2 ppm at pH 7, conductivity 1,030 μS/cm, UV light intensity 5,400 μW/cm^2, applied electrical potential 1.5 V, photoanode (TiO_2 nanotubes on Ti lath) and cathode (Ti) area: 2 cm×5 cm, feed volume 1,000 mL, the ratio of the number of photoanode : cathode=4 : 4, rotating speed 90 rpm).

anode in a solution of 1,030 μS/cm conductivity adjusted with NaCl. The LSV curves under light off (dark) show that the potential variation did not change the current flow. In contrast, a photocurrent increased with increasing applied positive electrical potentials (0-3.5 V *vs.* Ag/AgCl) under UV light irradiation. Moreover, the chronoamperometry results were consistent with the values of LSV results, as shown in Fig. 6(b). Under alternative light on/off condition at different electrical potentials (0-3.5 V *vs.* Ag/AgCl), high photocurrent was obtained with increasing voltages or close to zero currents. As previously mentioned, the optimum ranges of voltage were obtained. Therefore, extremely high electrical potential may be one reason to deteriorate the electrode stabilization [22].

5. Effect of UV Intensity and Number of Photoanode on MB Removal

The removal of MB was investigated with different numbers of photoanode (TiO_2 nanotubes on Ti lath) under UV illumination (Fig. 7). As expected, the degradation of MB was more effective with increasing numbers of rotating photoanodes. Where the four photoanodes with four cathodes were applied, the degradation efficiency of MB was relatively lower than that with the eight photoanodes and four cathodes because of a small quantity of TiO_2 on Ti lath or the insufficient dosages to obtain complete removal. Moreover, with increasing UV intensity (8,400 $\mu W/cm^2$) and number of photoanodes, the degradation rate of MB significantly increased than those at lower intensity and four photoanodes (Fig 7). This result can be explained by the fact that the high UV intensity increases the formation of reactive hydroxyl radicals on the surface of TiO_2 nanotubes. Some of the water treatment studies have also showed the relationship between light intensity and photoelectrocatalytic reaction [28,29].

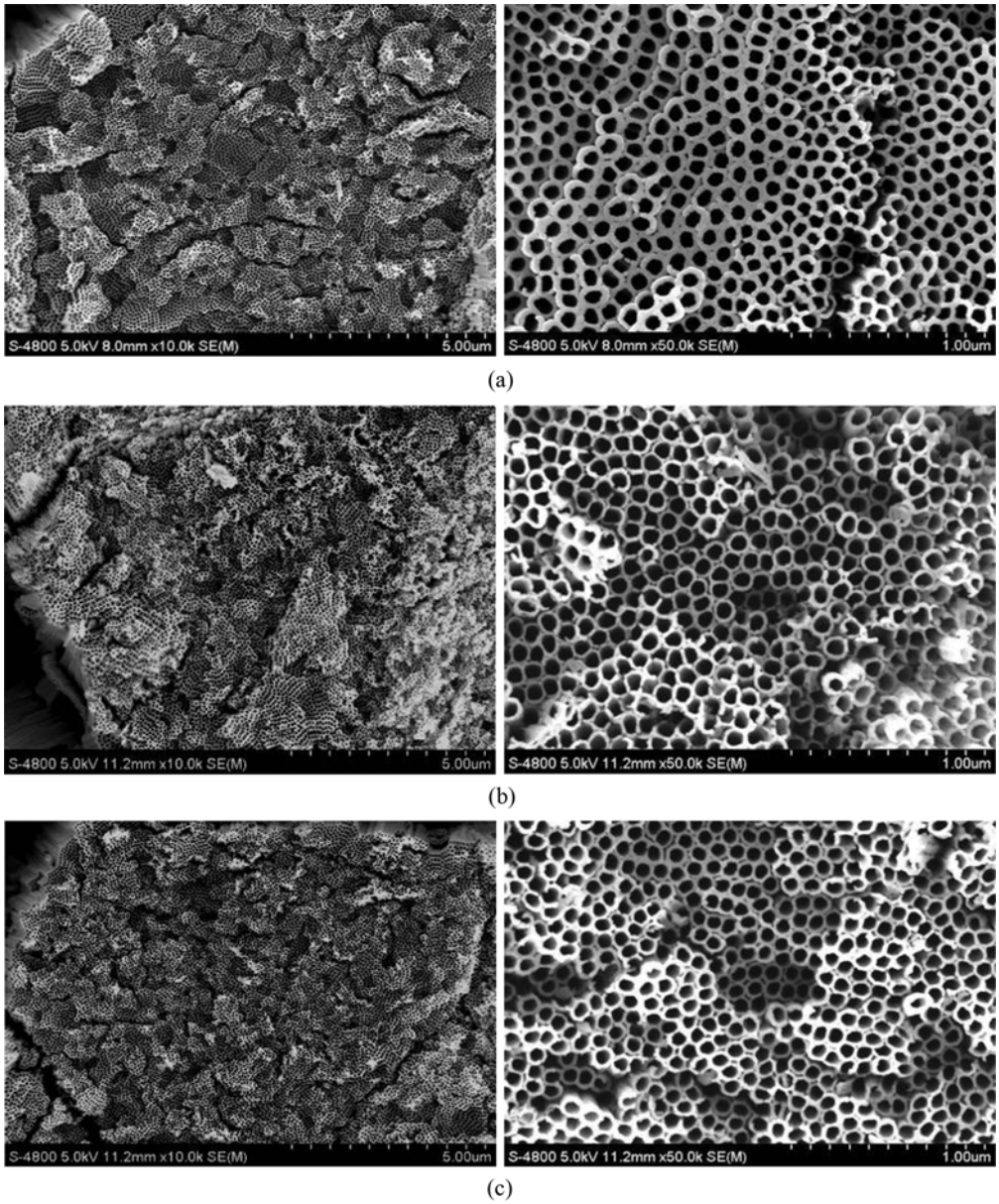

Fig. 9. SEM images of TiO_2 nanotubes on Ti lath; (a) before reaction (virgin); (b) after reaction at 1.5 V; (c) after reaction at 2.5 V.

6. Stability of TiO_2 Nanotubes/Ti Electrode

The stability of photoanode is an important factor to consider for the water treatment applications [4,19,30]. To examine the stability of the photoanode used in this study, five cycles of rotating photoelectrocatalytic process were repeated to remove MB at applied electrical potential (1.5 V and 2.5 V). One cycle was 6 hr and seven samples were measured for each experiment. The photoelectrocatalytic reactor including the electrodes was cleaned with pure water after each experiment. As shown in Fig. 8(a) and (b), the degradation profiles of the five repeating experiments at 1.5 and 2.5 V demonstrate the similar trends without deterioration in the photoelectrocatalytic activity. The average MB removal at 1.5 V and 2.5 V was 86.2±2.1% and 90.4±2.6%, respectively.

The selected SEM images of the photoanode are shown in Fig. 9. The first image (Fig. 9(a)) corresponds to the virgin sample before the photoelectrocatalytic reaction. The second and third images (Fig. 9(b) and (c)) are the samples after the repeated reaction at 1.5 V and 2.5 V, respectively. The TiO_2 nanotubes on Ti lath were not damaged and exhibited uniform morphological properties. In addition, the ICP-OES analyses of water samples were performed to determine the Ti detached from the TiO_2 nanotubes after the photoelectrocatalytic reactions at different voltages. Ti was not detected from all the samples, and the anodized nanotubular TiO_2 was well immobilized on the Ti lath without altering their structure.

CONCLUSIONS

We designed a new rotating photoelectrocatalytic reactor to enhance the removal efficiency of organic pollutant. The rotating photoelectrocatalytic reactor system consists of TiO_2 nanotubes on Ti lath and Ti lath as the photoanode and cathode, respectively, to apply electrical potential under UV irradiation. In particular, we investigated the effect of key parameters such as such applied electrical potential, UV intensity, rotating speed of electrodes on the degradation efficiencies of organic pollutant.

The photoelectrocatalytic reaction showed a better performance than the photocatalytic reaction for the oxidation of MB. Especially, the removal efficiency and reaction rate were significantly related to the rotating speed, with 90 rpm the optimum rotating speed in this system. In addition, the electrical potential in the range of 1.5-2.5 V was optimum for the degradation of MB in this system, and the results of photocurrent measurements indicated that the removal efficiency was slightly above the optimum range. In the photoelectrocalytic process, the UV intensity significantly affected the degradation of MB. The removal efficiencies of MB increased with increasing UV intensity. Five repeated tests of the TiO_2 nanotubes on the Ti lath showed a similar MB degradation, and no damage was observed on the surface at 1.5 V and 2.5 V applied electrical potential.

ACKNOWLEDGEMENTS

This work was carried out under the framework of Research and Development Program of the Korea Institute of Energy Research (B6-2422).

REFERENCES

1. R. Daghrir, P. Drougi and D. Robert, *J. Photochem. Photobiol. A: Chem.*, **238**, 41 (2012).
2. T. Ochiai and A. Fujishima, *J. Photochem. Photobiol. C: Photochem. Reviews*, **12**, 247 (2012).
3. M. A. Lazar, S. Varghese and S. S. Nair, *Catalysts*, **2**, 572 (2012).
4. A. Zhu, Q. Zhao, X. Li and Y. Shi, *Appl. Mater. Interf.*, **6**, 671 (2013).
5. X. Wang, L. Sun, S. Zhang and X. Wang, *Appl. Mater. Interf.*, **6**, 1361 (2014).
6. G. K. Mor, K. Shankar, M. Paulose, O. K. Varghese and C. A. Grimes, *Nano Lett.*, **5**, 191 (2005).
7. G. K. Mor, K. Shankar, M. Paulose, O. K. Varghese and C. A. Grimes, *Sol. Energy Mater. Sol. Cells.*, **90**, 2011 (2006).
8. M. Paulose, G. K. Mor, O. K. Varghese, K. Shankar and C. A. Grimes, *J. Photochem. Photobiol. A: Chem.*, **178**, 8 (2006).
9. S. Oh, W. Nam, H. Joo, S. Sarper, J. Cho, C. Lee and J. Yoon, *Solar Energy*, **85**, 2256 (2011).
10. J. Yoon, S. Bae, E. Shim and H. Joo, *J. Power Source*, **189**, 1296 (2009).
11. S. Bae, E. Shim, J. Yoon and H. Joo, *J. Power Source*, **185**, 439 (2008).
12. S. Bae, J. Kang, E. Shim, J. Yoon and H. Joo, *J. Power Source*, **179**, 863 (2008).
13. M. Park, A. Heo, E. Shim, J. Yoon, H. Kim and H. Joo, *J. Power Source*, **95**, 5144 (2010).
14. J. Yoon, E. Shim, S. Bae and H. Joo, *J. Hazard. Mater.*, **161**, 1069 (2009).
15. Y. Kim, H. Joo, N. Her, Y. Yoon, C. H. Lee and J. Yoon, *Chem. Eng. J.*, **229**, 66 (2013).
16. J. K. Im, J. Yoon, N. Her, J. Han, K. D. Zoh and Y. Yoon, *Sep. Purif. Technol.*, **141**, 1 (2015).
17. Y. Kim, H. Joo, N. Her, Y. Yoon, J. Sohn, S. Kim and J. Yoon, *J. Hazard. Mater.*, **288**, 124 (2015).
18. X. Hu, H. Ji, F. Chang and Y. Luo, *Catal. Today*, **224**, 33 (2014).
19. X. Quan, S. Yang, X. Ruan and H. Zhao, *Environ. Sci. Technol.*, **39**, 3770 (2005).
20. H. Song, J. Shang, J. Ye and Q. Li, *Thin Solids Films*, **551**, 158 (2014).
21. S. C. Hayden, N. K. Allam and M. A. El-Sayed, *J. Am. Chem. Soc.*, **132**, 14406 (2010).
22. Y. B. Xie and X. Z. Li, *J. Hazard. Mater.*, **198**, 526 (2006).
23. W. C. Lin, C. H. Chen, H. Y. Tang, Y. C. Hsiao, J. R. Pan, C. C. Hu and C. Huang, *Appl. Catal. B: Environ.*, **140-141**, 32 (2013).
24. K. Cho and M. R. Hoffmann, *Chem. Mater.*, **27**, 2224 (2015).
25. C. A. Martinez-Huitle and S. Ferro, *Chem. Soc. Rev.*, **35**, 1324 (2006).
26. J. Li, L. Zheng, L. Li, Y. Xian and L. Jin, *J. Hazard. Mater.*, **139**, 72 (2007).
27. I. K. Konstantinou and T. A. Albanis, *Appl. Catal. B: Environ.*, **49**, 1 (2004).
28. N. Wang, X. Li, Y. Wang, X. Quan and G. Chen, *Chem. Eng. J.*, **146**, 30 (2009).
29. M. N. Chong, B. Jin, C. W. K. Chow and C. Saint, *Water Res.*, **44**, 2997 (2010).
30. Y. Xu, Y. He, X. Cao, D. Zhong and J. Jia, *Environ. Sci. Technol.*, **42**, 2612 (2008).